Bioorganic & Medicinal Chemistry Letters 21 (2011) 5487–5492

Contents lists available at ScienceDirect

Bioorganic & Medicinal Chemistry Letters

journal homepage: www.elsevier.com/locate/bmcl

Structure-based design and optimization of potent renin inhibitors on 5- or 7-azaindole-scaffolds

Hans Matter [a,*], Bodo Scheiper [a], Henning Steinhagen [a,†], Zsolt Böcskei [b], Valérie Fleury [c], Gary McCort [c]

[a] Sanofi-Aventis Deutschland GmbH, Chemical and Analytical Sciences, Building G878, D-65926 Frankfurt, Germany
[b] Sanofi-Aventis, Chemical and Analytical Sciences, 16, Rue d'Ankara, F-67080 Strasbourg, France
[c] Sanofi-Aventis, Cardiovascular Department,1, Avenue Pierre Brossolette, F-91385 Chilly-Mazarin, France

ARTICLE INFO

Article history:
Received 9 May 2011
Revised 24 June 2011
Accepted 26 June 2011
Available online 2 July 2011

Keywords:
Renin
Azaindole
Structure-based-design
Aspartyl-protease

ABSTRACT

The selective inhibition of the aspartyl protease renin is of high interest to control hypertension and associated cardiovascular risk factors. Following on preceding contributions, we report herein on the optimization of two series of azaindoles to arrive at potent and non-chiral renin inhibitors. The previously discovered azaindole scaffold was further explored by structure-based drug design in combination with parallel synthesis. This results in the identification of novel 5- or 7-azaindole derivatives with remarkable potency for renin inhibition. The best compounds on both series show IC_{50} values between 3 and 8 nM.

The control of hypertension can considerably reduce the risk of cardiovascular diseases like myocardial infarction, stroke, heart failure and end-stage kidney disease.[1,2] The endocrine renin-angiotensin system (RAS), regulating blood pressure and fluid electrolytes,[3] is one of the major and most intensively studied systems affecting the arterial blood pressure in humans. The aspartyl protease renin is released after activation of this system and then produces angiotensin I in a rate-limiting step. Consequently the inhibition of this step is perceived as effective antihypertensive strategy[4], causing multiple research groups to optimize novel series of renin inhibitors with oral bioavailability for medical therapy. Aliskiren (SPP100) is today the first molecule of this class, which has reached the market.[5]

In two recent contributions we reported on novel classes of non-chiral indole-3-carboxamides[6] and derived 4- and 6-azaindoles[7] as renin inhibitors. The combination of various phenylether or benzyl-substituents directed towards the renin lipophilic S1 pocket combined with adequate decoration at the indole or azaindole scaffold resulted in significant improvement of binding affinity. The best compounds from this study **1a–c** display IC_{50} values of 0.002 or 0.003 μM, respectively (Fig. 1). In this publication we describe the discovery, structure–activity-relationship and optimization of 5- or 7-azaindole-3-carboxamides as renin inhibitors, which are derived by structure-based design in combination with efficient parallel synthesis.

The superposition of X-ray crystal structures of our lead structures **1a** and **1c** in complex with renin (PDB 3OOT and 3SFC, Fig. 2)[6,7] reveals similar binding modes, thus forming a basis for structure-based design. Hydrogen-bonds are observed from the piperazine nitrogen to side chains of Asp^{32} and Asp^{215}, for the carboxamide oxygen to Thr77-OγH and for either the OH group directly or the 6-azaindole nitrogen indirectly contacting the flexible His^{287} side chain. Both phenyl rings at the indole N^1- and C^2-position are involved in lipophilic interactions to their corresponding subpockets.

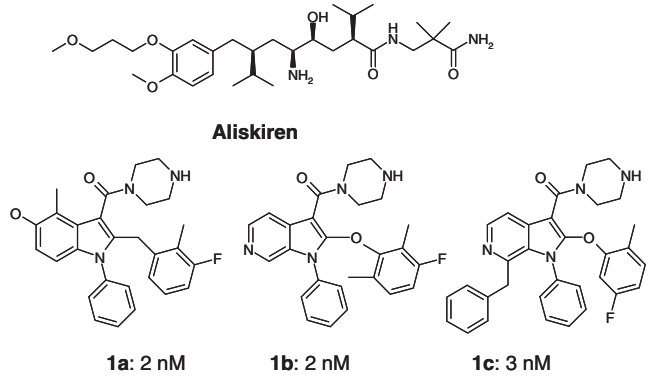

Figure 1. Chemical structures of indole-3-carboxamide **1a** and 6-azaindoles **1b** and **1c** as potent renin inhibitors.

* Corresponding author. Tel.: +49 69 305 84329.
E-mail address: Hans.Matter@sanofi-aventis.com (H. Matter).
† Present address: Grünenthal Pharma GmbH, Global Drug Discovery, Zieglerstr. 6, 52099 Aachen, Germany.

0960-894X/$ - see front matter © 2011 Published by Elsevier Ltd.
doi:10.1016/j.bmcl.2011.06.112

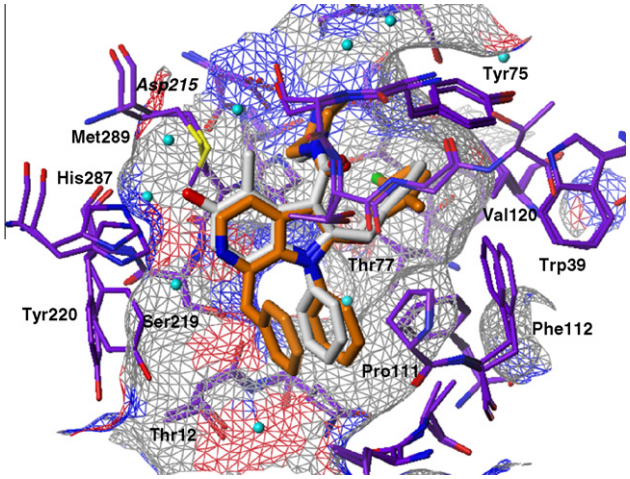

Figure 2. Superimposed X-ray structures of indole **1a** (PDB 3OOT, white carbon atoms, 2.5 Å resolution) and 6-azaindole **1c** (PDB 3SFC, orange carbon atoms, 2.1 Å resolution) in complex with human renin. The binding site from the **1a** complex is shown as MOLCAD[9] hydrogen bonding surface. Crystallographic water is indicated by cyan spheres.

In particular a relevant CH–π interaction to Tyr[75] is observed in the S1 pocket as important contribution to affinity. The 3-fluorine substituent is situated in a lipophilic subpocket close to the Asp[32] carboxylate, while the orientation of the 5-methyl substituent differs.[7] In contrast to **1a**, the 5-methyl group in **1c** points towards the opposite site of the S1 pocket, thus contacting side chains of Pro[111] and Phe[112], although dihedral angles of phenoxy- or benzyl substituents differ by only 8°. The 7-benzyl-substituent at the 6-azaindole is oriented towards the more open binding site region, contacting the side chains of Pro[111] and Leu[114]. Furthermore this ring is engaged in an intramolecular π–π interaction[8] to the azaindole-N^1-phenyl ring, thus stabilizing the bioactive conformation.

Our previous discovery of potent 4- or 6-azaindoles with lower lipophilicity prompted us to explore other scaffolds with respect to renin activity. Docking[10–12] suggested either 5- or 7-positions at the indole core to be suitable for introducing nitrogen atoms, which leads to frameworks orienting the privileged indole side chains towards appropriate subpockets. In particular we investigated the possibility to form favorable polar interactions to the binding site, thus for example to His[287] imidazole, either directly or via conserved water. This substitution will also modulate physicochemical properties like lipophilicity of the lead series, which might affect pharmacokinetic properties.

The synthetic pathway for the preparation of the 5- and 7-azaindole derivatives **3**–**7** is outlined in Scheme 1 for examples **5b** and **5g**. The 5-azaindole **2a** was arylated under Copper catalysis[13], then oxidized with bromine and subsequently reduced according to the procedure of Robinson.[14] Vilsmeier–Haack formylation with concomitant chlorination yielded aldehyde **2b**. Oxidation to the acid and coupling with *N*-Boc-piperazine provided key intermediate **2c**. The chloride **2c** was then either coupled in a Palladium-mediated reaction followed by deprotection to the corresponding benzyl derivative **5g** or submitted to nucleophilic substitution to provide the arylether derivative **5b** after cleavage of the protecting group under acidic conditions. The synthesis of all other derivatives **3** to **7** was carried out accordingly to this scheme. All substituted piperazine derivatives for compound series **7** were commercially available; *N*-Boc was also employed as protecting group.

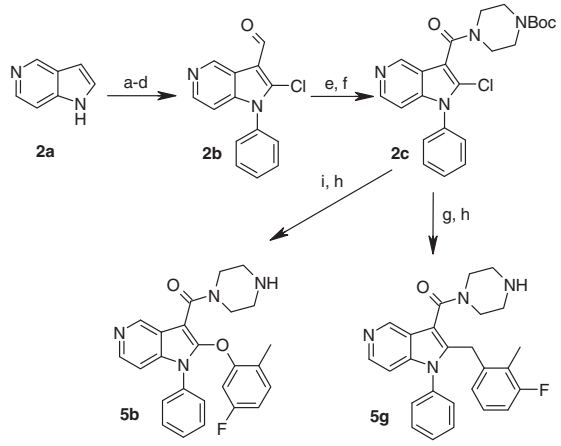

Scheme 1. Reagents and condition: Synthesis of compounds **5b** and **5g**. Reagents: (a) Phenyl iodide, CuI,(1*S*,2*S*)-(+)-Diaminocyclohexane, K_3PO_4, dioxane, 110 °C, 99%; (b) Br_2, *t*-BuOH, H_2O, rt; (c) Pd/C, H_2, EtOH, rt; (d) (i) $POCl_3$, DMF, DCM, pyridine, 0 °C→rt, (ii) $POCl_3$, 100 °C, 28% over three steps; (e) $NaClO_2$, NaH_2PO_4, *t*-BuOH, rt, quant.; (f) *N*-Boc-piperazine, TOTU, NMM, DMF, rt, 44%; (g) (i) 3-Fluoro-2-methylbenzylbromide, Zn, THF, 0 °C, (ii) 9-MeO-9-BBN, −78 °C→rt, (iii) $Pd(OAc)_2$, S-Phos, DMF, 100 °C, 26%; (h) TFA, DCM, rt, quant.; (i) 5–Fluoro-2-methylphenol, NaH, NMP, rt→140 °C, microwave, 77%.

Table 1
In vitro activity for compounds **3a–3i**[a]

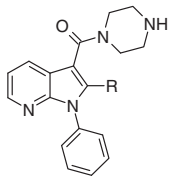

Compds	*R*	Renin IC_{50} (μM)
3a		1.830
3b		0.098
3c	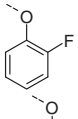	5.06
3d	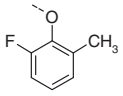	0.231
3e	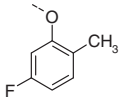	0.396
3f	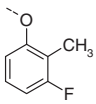	0.17
3g	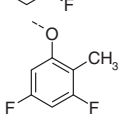	0.504
3h	Benzyl	6.410
3i	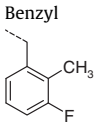	0.086

[a] IC_{50} data were obtained as described in the text and in Ref. 16.

Table 2
In vitro activity for compounds **4a–4i**[a]

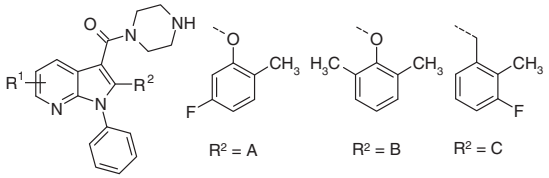

Compds	R^1	R^2	Renin IC_{50} (μM)
4a	5-OH	A	0.006
4b	5-OH	C	0.006
4c	5-OCH_3	C	4.670
4d	6-OCH_3	A	0.015
4e	6-OCH_3	B	0.003
4f	4-Ethyl	A	1.230
4g	4-Ethyl	C	0.089
4h	4-Propyl	A	1.850
4i	4-Propyl	B	0.186
4j	4-Propyl	C	0.218

[a] IC_{50} data were obtained as described in the text and in Ref. 16.

First we decorated the 7-azaindole scaffold[15] using privileged[6,7] phenylether- and benzyl-derivatives. A representative set of compounds is shown in Table 1 with experimental IC_{50} values (μM). To calculate IC_{50} values, the activity of an inhibitor was evaluated in a 10 point concentration range, in duplicate (intraplate).[6,7,15,16] Two to four independent experiments were performed. The IC_{50} is expressed as geometric mean ± standard deviation (SD). The standard deviation was low for this assay.

The substituents in Table 1 are oriented towards the lipophilic renin S1 pocket to exploit the CH–π interaction to Tyr75 and the affinity gain by addressing appropriate subpockets. Variations of the aromatic ring in S1 then resulted in improved affinity compared to the lead **3a** with a phenoxy-group and an IC_{50} value of 1.830 μM, as also expected from optimizing the indole and 4- or 6-azaindole structures.[6,7] Comparing **3a** with its related indole shows a fourfold better activity for the indole (0.420 μM).[6] Adding an *ortho*-methyl group to the phenoxy-ring resulted in compound **3b** as most active derivative from the arylether-series with an IC_{50} value of 0.098 μM and thus a fivefold lower affinity as for the indoles (0.021 μM).[6] The addition of fluorine in ortho position to **3a** or **3b** does not improve affinity (**3c**, 5.06 μM; **3d**, 0.231 μM).

As for the phenylether subseries, the corresponding S1-directed benzyl-substituents also exhibit consistently weaker affinity, when comparing the 7-azaindole derivatives to the indole series.[6] The unsubstituted benzyl-derivative is about 70-fold less active in the 7-azaindole series (**3h**, 6.410 μM), while the addition of *ortho*-methyl-meta-fluoro-substituents to the benzyl ring resulted in **3i** with an IC_{50} value of 0.086 μM, thus being twofold more active as the 2-phenoxy-7-azaindole-derivative **3f**. However, its significantly lower activity compared to the indole, 4-or 6-azaindole scaffolds was unexpected (six to nine fold lower affinity).

The inspection of the X-ray crystal structure of **1a** with renin plus docking of selected 7-azaindoles led us to decorate the 7-azaindole using adequate substituents. From Table 1 and our previous SAR investigations, we identified three adequate S1-directed phenoxy- and benzyl-moieties for further systematic variations. Those moieties are shown in Table 2 (R^2 = A, B or C) together with a selection of renin inhibitors from this optimization. First we introduced a small-polar 5-hydroxy group, directed towards the His^{287} side chain to allow for hydrogen-bond interactions, in particular as hydrogen-bond donor to His^{287}.

The corresponding derivatives **4a** and **4b** with 5-OH groups at the 7-azaindole scaffold were highly active with IC_{50} values of 0.006 μM each. However, the addition of a 5-methoxy substituent resulted in **4c** with an IC_{50} value of 4.670 μM, which could be explained by the lacking hydrogen-bond donor at this position plus additional increased steric bulk.

However, shifting the methoxy substituent to position 6 at the 7-azaindole resulted in very potent compounds, exemplified by **4d**

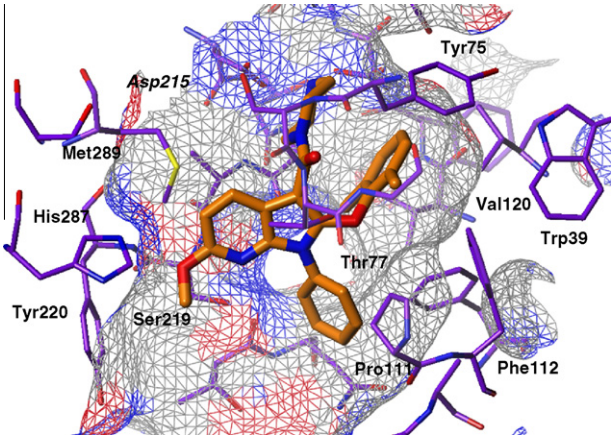

Figure 3. Binding pose of compounds **4e** (upper: orange carbons) from docking into the renin binding site from the X-ray crystal structure of **1a**.

Table 3
In vitro activity for compounds **5a–5h**[a]

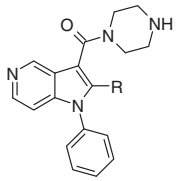

Compds	*R*	Renin IC_{50} (μM)
5a		0.847
5b	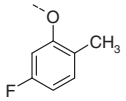	0.123
5c	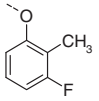	0.181
5d	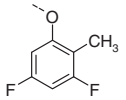	0.65
5e	Benzyl	3.4
5f	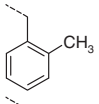	0.520
5g	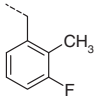	0.008
5h	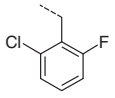	0.10

[a] IC_{50} data were obtained as described in the text and in Ref. 16.

(0.015 μM) and **4e** (0.003 μM). The compatibility of this binding site region with larger and more lipophilic substituents like methoxy is in agreement to our previous SAR investigations at the indole scaffold.[6] Interestingly the analogous indoles to **4d** and **4e** are two to four fold less active with IC_{50} values of 0.024 μM and 0.012 μM, respectively.

The binding mode of **4e** in the renin binding site from docking in Figure 3 suggests a highly similar binding mode compared to X-ray structures of related inhibitors. Characteristic interactions essential for high-affinity binding are preserved, so for example the piperazine-aspartate interactions as well as the bifurcated hydrogen bond from the indole-3-carboxamide carbonyl to Thr77-OγH (distance 1.8 Å) and NH (2.2 Å). The 6-methoxy-substituent is situated in a more open binding site region surrounded by the aromatic rings of His^{287} and Tyr^{220}. Interestingly the ether oxygen is only around 2.8–2.9 Å apart from the backbone amide protons of Ser^{219} and Tyr^{220}. Hence, those might potentially serve as H-bond donors for this relatively weak acceptor, while the distance is outside the usual range for this interaction. In related X-ray structures, structurally conserved water molecules are present in this area, although often not close to the donors. In addition the methoxy-oxygen is 3.6 Å away from the Ser^{219}—OγH in this flexible side chain, which also favors hydrogen bond interactions. The lipophilic methoxy carbon in directed towards the plane of the aromatic Tyr^{220} side chain with a distance of 4.2 Å to the nearest aromatic carbon.

Although the further analysis of our X-ray structures suggested that lipophilic substituents in position 4 of the 7-azaindole scaffold might be favorable for affinity, the introduction of both an ethyl or propyl-side chain did not result in an increase of affinity. While **4f** with a 4-ethyl substituent and a 2-methyl-5-fluoro-phenylether substituent has an IC_{50} value of 1.230 μM, the corresponding 2-methyl-3-fluoro-benzyl substituted **4g** shows an IC_{50} value of 0.089 μM, respectively. Hence for the benzyl series, the renin affinity is related to the unsubstituted **3i**, while in the phenylether subseries, there was a significant loss of affinity, when comparing to **3e**. The larger 4-propyl substitution now resulted in derivatives with lower affinity (**4j**, 0.218 μM).

Next we explored a related set of S1-directed phenylether- and benzyl variations at a 5-azaindole structure[15] in order to evaluate, whether the more polar aromatic nitrogen in this position could have a positive influence due to hydrogen-bonding in this area of the binding site as well as to general physicochemical properties. The representative set of derivatives is shown in Table 3. Consistently with other series, the 2-methyl-5-fluoro-phenylether substituent leads to the highly active compound **5b** for the phenylether subseries with an IC_{50} value of 0.123 μM. Hence, the binding affinity is higher for this S1 substituent in the 5-azaindole series compared to the 7-azaindoles (**3e**, 0.396 μM), while for the indole scaffold, an affinity of 0.005 μM was observed (entry **2j** in Ref.6).

This finding is similar for the benzyl-subseries. While for the 5-azaindoles the best affinity in Table 3 was observed for the 2-methyl-3-fluoro-benzyl substituent directed to S1 (**5g**, 0.008 μM), the affinity is lower for the 7-azaindole (**3i**, 0.086 μM). Interestingly for this case, the corresponding indole derivative is equipotent to **5g** (entry **2n**, 0.009 μM in Ref. 6).Summarizes our investigation to add 6-hydroxy- or 6-methoxy substitutions to the 5-azaindole. In addition we replaced the aromatic azaindole N^1-phenyl substituent against a larger cyclohexyl-substituent. The computational investigation of tautomer ratios for 6-hydroxy-5-azaindoles suggested the pyridone-form to be exclusively present in solution.[17] This pyridone would thus allow the 5-amide-hydrogen to act as H-bond donor for His^{287}. The corresponding derivative **6d** is more active than the unsubstituted 5-azaindole **5b** (0.024 versus 0.123 μM). Replacing the 5-OH group versus a 5-methoxy-group, which does not form a pyridone tautomer, is found to be slightly less active (**6c**, 0.073 μM). Interestingly, this SAR trend is reversed, when comparing these changes for the 2-methyl-3-fluoro-benzyl substituents.

Table 4
In vitro activity for compounds **6a–6i**[a]

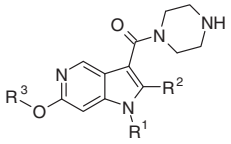

Compds	R^1	R^2	R^3	Renin IC_{50} (μM)
6a	Cy	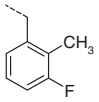	CH_3	0.150
6b	Ph	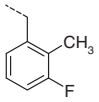	CH_3	0.006
6c	Ph	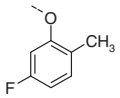	CH_3	0.073
6d	Ph	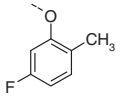	H	0.024
6e	Cy	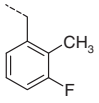	H	0.116
6f	Ph	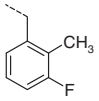	H	0.088
6g	Cy	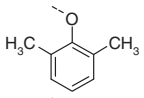	CH_3	0.099
6h	Cy	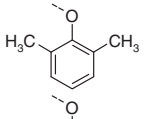	H	0.080
6i	Cy	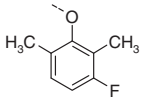	H	0.098

[a] IC_{50} data were obtained as described in the text and in Ref. 16.

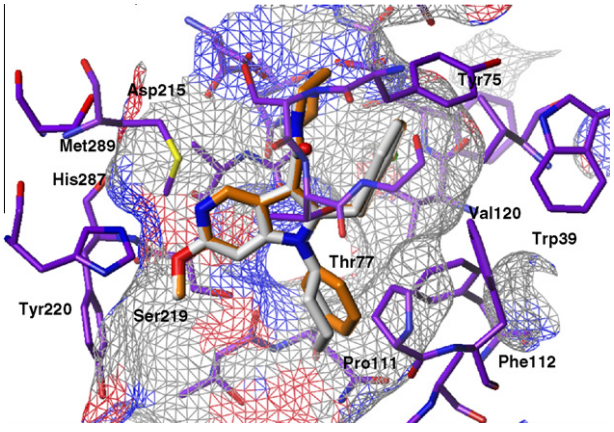

Figure 4. Binding poses of compounds **6b** (orange carbons) and **6a** (white carbons) from docking into the renin binding site from the X-ray crystal structure of **1a**.

Here the derivative **6b** with a 6-methoxy-5-azaindole core and an IC_{50} value 0.006 μM is significantly more active as the pyridone **6f** (0.088 μM). This preference for small lipophilic methoxy-substituents in the 6-position has also been observed for the corresponding 4-azaindole derivatives (c.f. **4e**, 0.003 μM).

The replacement of the N^1-phenyl-ring against the larger cyclohexyl (R^1 = Cy in Table 4) results in reduced affinity, when comparing **6b** to **6a** with IC_{50} values of 0.006 and 0.150 μM, respectively. The binding mode for both derivatives in Figure 4 from docking suggests a better fit of the aromatic N1-substituent in **6b** in the S3 pocket, which is lined also by the aromatic ring of Phe[112]. The distance of both centroids is 5.1 Å, which also suggest some involvement from π−π interactions in this S3 pocket. In contrast, the cyclohexyl-group, although situated in a lipophilic environment, is oriented more towards the open space of the pocket due to steric constraints.

For the pyridone-derivative, this decrease in affinity is less dramatic, when comparing **6f** (0.088 μM) to **6e** (0.116 μM). This lower renin affinity, however, is still consistent with observations for the other scaffolds underscoring the hydrophobic nature of this interaction in the renin S3-subpocket. Obviously this increased size of the N^1-substituent is compatible with only some substitution motifs, while other motifs might alter the overall binding mode, thus repositioning this group in S3. We then evaluated N^1-cyclohexyl derivatives at the 6-hydroxy-5-azaindole scaffold further by adequate S1-directed phenylether substituents.

Active compounds were obtained for example using a 2,6-dimethyl-phenylether (**6h**, 0.080 μM) or a 3-fluoro-2,6-dimethyl-phenylether motif (**6i**, 0.098 μM). Replacing the 6-OH, which again is present in its pyridone tautomeric form, by a 6-methoxy-substituent does not significantly affect binding affinity (**6g**, 0.099 μM), as observed for **6d** (0.024 μM, see above).

This N1-cyclohexyl-6-hydroxy-5-azaindole scaffold was also chosen to explore variations at the piperazine substructure. Representative examples are summarized in Table 5 with *R*1 = A, B or C indicating the S1-directed substituents. These chiral substitutions at the piperazine were introduced after comparing the X-ray structure of Aliskiren (PDB 2V0Z) to the indole binding pose.[18] The bond vector connecting the Aliskiren aminoethanol to its isobutyl-carboxyamide directed towards the renin S1′-pocket is aligned with the vector C2-Hpro-S next to the secondary amine function. Chiral lipophilic piperazine substitutions directed towards the renin S1′ pocket could also impact affinity.

Introducing the lipophilic S-methyl substituent at this scaffold thus resulted in the potent derivatives **7a** (0.011 μM) and **7b** (0.037 μM). Comparing **7b** to its parent structure **6i** reveals a threefold increase in affinity by this chiral methyl group. However, such an improvement was not observed for the benzyl subseries. Here the derivative **7d** (0.154 μM) is slightly less potent as the parent compound **6e** (0.116 μM), again indicating a nonlinear SAR between the phenylether- and benzyl-subseries. Replacing the 6-OH group against a 6-methoxy-group in **7c** resulted in lower affinity (**7c**, 0.32 μM), in agreement to observations for the parent molecule **6e** (0.116 μM) versus **6a** (0.150 μM), respectively. The renin affinity was lower in general, if the chain length of the substituent was increased by adding a methoxy- or hydroxyl-substitution, as exemplified in derivatives **7e–g** with IC_{50} values ranging from 1.1 to 4.09 μM, respectively.

Table 5
In vitro activity for compounds **7a–7g**[a]

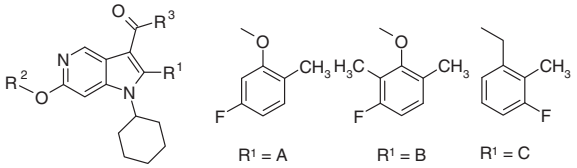

Compds	R^1	R^2	R^3	Renin IC_{50} (μM)
7a	A	H	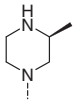	0.011
7b	B	H	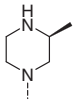	0.037
7b	C	CH_3	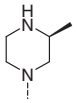	0.32
7d	C	H	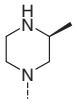	0.154
7e	C	CH_3	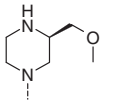	4.09
7f	C	CH_3	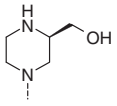	3.26
7g	C	H	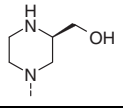	1.1

[a] IC_{50} data were obtained as described in the text and in Ref. 16.

Selected compounds were further profiled with IC_{50} values in human or mouse plasma, Caco-2 permeability and physicochemical data[19] (Table 6). The best compounds display IC_{50} values between 3 and 8 nM with only slight activity reduction by adding human or mouse plasma. The Caco-2 Papp value for **6b** on the 5-azaindole scaffold furthermore suggests its potential for significant intestinal absorption.

In summary we have reported the design and structure–activity relationship of novel series of potent renin inhibitors based on 5- or 7-azaindole scaffolds. Both scaffolds were developed further after analysis of previous indole-3-carboxamides, 4- and 6-azaindoles. In general structure-activity trends are correlated, while

Table 6
Further profiling of selected Renin inhibitors[a]

Compds	Renin IC_{50} (μM)	Renin IC_{50} with human plasma (μM)	Renin IC_{50} with mouse plasma (μM)	Caco-2 Permeability (*10−7 cm/s)	log *P* (MoKa)	pKa (basic, MoKa)	log *D* (pH 7.4, MoKa)	Ligand efficiency	Lipophilic ligand efficiency
4a	0.006	0.189	0.057	4.5	1.9	8.1	−0.5	0.34	6.32
4b	0.006	0.095	0.159	nd	2.5	8.4	−0.1	0.34	5.72
5g	0.008	0.200	0.410	6.4	2.5	8.1	1.7	0.34	5.60
6b	0.006	0.328	0.364	22	3.2	8.1	2.4	0.33	5.02

[a] Data were obtained as described Ref. 19; nd = not determined.

there is no strict linearity when transferring preferred substituents. Hence, we explored both novel scaffolds with a privileged set of building blocks directed to S1 in addition with other modifications at the azaindole N^1-position, the piperazine and the azaindole-6-position.

After decoration of these scaffolds, compounds with high affinity and favorable physicochemical properties were identified. In particular, the incorporation of substituted phenoxy- or benzyl derivatives in S1 combined with substitution at the azaindole core led to a significant improvement of affinity. The availability of X-ray structures of renin-inhibitor complexes during our optimization allowed us to unveil the key determinants to affinity.

Acknowledgments

The authors would like to thank Sabrina Berger, Holger Gaul, Silvia Hein, Laetitia Martin, Andrea Müller, Mathilde Pierre and Katja Wittmann for their technical assistance.

References and notes

1. Kearney, P. M.; Whelton, M.; Reynolds, K.; Muntner, P.; Whelton, P. K.; He, J. *Lancet* **2005**, *365*, 217.
2. (a) Amin Zaman, M.; Oparil, S.; Calhoun, D. A. *Nat. Rev. Drug Disc.* **2002**, *1*, 621; (b) Jensen, C.; Herold, P.; Brunner, H. R. *Nat. Rev. Drug Disc.* **2008**, *7*, 399.
3. MacGregor, G. A.; Markandu, N. D.; Roulston, J. E.; Jones, J. E.; Morton, J. J. *Nature* **1981**, *291*, 329.
4. Wood, J. M.; Stanton, J. L.; Hofbauer, K. G. *J. Enzyme Inhib. Med. Chem.* **1987**, *1*, 169.
5. (a) Göschke, R.; Stutz, S.; Rasetti, V.; Cohen, N.-C.; Rahuel, J.; Rigollier, P.; Baum, H.-P.; Forgiarini, P.; Schnell, C. R.; Wagner, T.; Grütter, M. G.; Fuhrer, W.; Schilling, W.; Cumin, F.; Wood, J. M.; Maibaum, J. *J. Med. Chem.* **2007**, *50*, 4818; (b) Maibaum, J.; Stutz, S.; Göschke, R.; Rigollier, P.; Yamaguchi, Y.; Cumin, F.; Rahuel, J.; Baum, H.-P.; Cohen, N.-C.; Schnell, C. R.; Fuhrer, W.; Grütter, M. G.; Schilling, W.; Wood, J. M. *J. Med. Chem.* **2007**, *50*, 4832.
6. Scheiper, B.; Matter, H.; Steinhagen, H.; Stilz, U.; Böcskei, Z.; Fleury, V.; McCort, G. *Bioorg. Med. Chem. Lett.* **2010**, *20*, 6268.
7. Scheiper, B.; Matter, H.; Steinhagen, H.; Böcskei, Z.; Fleury, V.; McCort, G. Bioorg. Med. Chem. Lett. **2011**, *21*, in press. doi:10.1016/j.bmcl.2011.06.114.
8. (a) Burley, S. K.; Petsko, G. A. *Science* **1985**, *229*, 23; (b) McGaughey, G. B.; Gagné, M.; Rappé, A. K. *J. Biol. Chem.* **1998**, *273*, 15458.
9. Heiden, W.; Goetze, T.; Brickmann, J. *J. Comp. Chem.* **1993**, *14*, 246.
10. McMartin, C.; Bohacek, R. S. *J. Comput.-Aided Mol. Des.* **1997**, *11*, 333.
11. Friesner, R. A.; Banks, J. L.; Murphy, R. B.; Halgren, T. A.; Klicic, J. J.; Mainz, D. T.; Repasky, M. P.; Knoll, E. H.; Shelley, M.; Perry, J. K.; Shaw, D. E.; Francis, P.; Shenkin, P. S. *J. Med. Chem.* **2004**, *47*, 1739.
12. Modeling was done using Sybyl 8.0 (Tripos) employing the MMFF94s force field (Halgren, T. J. *Comp. Chem.* **1999**, *20*, 720.). Protein–ligand complexes were minimized using the quasi-Newton–Raphson procedure. For manual docking, ligands were placed in the binding site and optimized treating all side chains within 4 Å flexible. Automated docking was done using QXP[10] or Glide.[11]
13. Filipski, K. J.; Kohrt, J. T.; Casimiro-Garcia, A.; Van Huis, C. A.; Dudley, D. A.; Cody, W. L.; Bigge, C. F.; Desiraju, S.; Sun, S.; Maiti, S. N.; Jaber, M. R.; Edmunds, J. J. *Tetrahedron Lett.* **2006**, *47*, 7677.
14. Robinson, R. P.; Donahue, K. M. *J. Org. Chem.* **1991**, *56*, 4805.
15. Steinhagen, H.; Scheiper, B.; Matter, H.; McCort, G. WO 2009095162; PCT Int. Appl. **2009**.
16. Inhibitory activity expressed as inhibition constant IC_{50} toward recombinant human renin was determined using an assay in which the non-endogenous fluorogenic substrate Dabcyl-γ-Abu-Ile-His-Pro-Phe-His-Leu-Val-Ile-His-Thr-EDANS is cleaved at the Leu-Val bond in analogy to angiotensinogen. Human renin at a concentration of 5 nM is incubated with the test compound at various concentrations and the substrate at a concentration of 10 μM (2 h at rt) in 0.05 M Tris buffer (pH 8). The increase in fluorescence due to fluorescence resonance energy transfer at an emission wavelength of 485 nM is recorded in a microplate spectrofluorometer.[15]
17. Tautomer ratios were computed using the Tauthor approach, as implemented in MoKa (Molecular Discovery Ltd., version 1.1.0): Milletti, F.; Storchi, L.; Sforna, G.; Cross, S.; Cruciani, G. *J. Chem. Inf. Model.* **2009**, *49*, 68.
18. Rahuel, J.; Rasetti, V.; Maibaum, J.; Rüeger, H.; Göschke, R.; Cohen, N.-C.; Stutz, S.; Cumin, F.; Fuhrer, W.; Wood, J. M.; Grütter, M. G. *Chem. Biol.* **2000**, *7*, 493.
19. a Recombinant human renin is incubated with the inhibitor at various concentrations plus the substrate Dabcyl-γ-Abu-Ile-His-Pro-Phe-His-Leu-Val-Ile-His-Thr-EDANS at 25 μM for 30 min at 37 C and 30 min at rt in human or mouse (C57BL6) plasma. Fluorescence is recorded at an excitation wavelength of 330 nM and an emission wavelength of 485 nM. IC_{50} values are calculated from inhibition as function of concentration from multiple measurements.; b Permeability studies using Caco-2/TC7 cells are performed using 20 μM compound concentration in the apical to basolateral direction with a pH gradient (6.5–7.4) and a BSA gradient (0.5–5%). After 2 h at 37 °C, the apparent permeability value (Papp) is obtained from quantification [$^{*}10^{-7}$ cm/s].; Physico-chemical properties (pKa, log *P*, log *D*) are computed using MoKa (Molecular Discovery Ltd., version 1.1.0.): (c) Milletti, F.; Storchi, L.; Sforna, G.; Cruciani, G. *J. Chem. Inf. Model.* **2010**, *47*, 2172; Ligand and lipophilic ligand efficiencies are computed according to: (d) Hopkins, A. L.; Groom, C. R.; Alex, A. *Drug Disc. Today* **2004**, *9*, 430; Leeson, P. D.; Springthorpe, B. *Nat. Rev. Drug Disc.* **2007**, *6*, 881.